# Interactions between lattice dislocations and grain boundaries in L12 ordered compounds investigated by in situ transmission electron microscopy and computer modelling experiments

Hosson, J.Th.M. de; Pestman, B.P.

*Published in:*
Materials Science and Engineering%3A A

*DOI:*
10.1016/0921-5093(93)90704-I

# Interactions between lattice dislocations and grain boundaries in $L1_2$ ordered compounds investigated by *in situ* transmission electron microscopy and computer modelling experiments

J. Th. M. de Hosson and B. P. Pestman

*Department of Applied Physics, Materials Science Center, University of Groningen, Nijenborgh 4, 9747 AG Groningen (Netherlands)*

**Abstract**

In this paper the interaction between lattice dislocations and grain boundaries in $Ni_3Al$ is reported as investigated by means of *in situ* transmission electron microscopy deformation experiments and modelling experiments. In particular, the interaction between screw dislocations and a coherent twin boundary was analysed in detail. The results of the *in situ* straining indicate that $\langle 110 \rangle$ screw dislocations impinging on a $\Sigma = 3$ coherent twin boundary, which have a Burgers vector parallel to the grain boundary plane, can be transmitted to the symmetric slip plane in the other grain under the influence of an applied stress. A one-to-one comparison with the results of a computer modelling study of exactly the same system in $Ni_3Al$ can be made and the experiment agrees with the simulations.

## 1. Introduction

Most metals with an f.c.c. structure are *ductile* and their strength *decreases* with *increasing* temperature. In contrast, intermetallic ordered compounds with $L1_2$ structure (space group $Pm3m$) show many remarkable and unusual mechanical properties. For example, many exhibit a temperature anomaly: a *rise* in their strength with *increasing* temperature, up to many hundreds of degrees celsius. In addition to strength at high temperatures, the moderate strength at lower temperatures gives the additional advantage that shaping at room temperature is relatively easy. These properties, together with the chemical resistivity that most ordered compounds show, make this class of materials very versatile for applications in hostile environments. In general these materials are very attractive for high temperature applications. However, although many of the ordered compounds with strong ordering tendency are ductile as single crystals, they show *brittle* fracture in their *polycrystalline* form. As a matter of course this hampers considerably their application.

$Ni_3Al$, with $L1_2$ structure, is one of the ordered compounds that is a very promising candidate for various applications such as turbine blades used by the aircraft industry [1]. If useful structural materials based on these intermetallic ordered compounds are ever to be developed further, it is crucial to scrutinize the reasons for their brittle behaviour. A possible reason could be low cohesion of the grain boundaries. If the energy of a grain boundary is not much lower than the sum of the energies of the two surfaces that are created by fracturing along the grain boundaries, intergranular fracture can occur by simple decohesion of the grain boundary.

This paper, however, deals with a different approach, considering explicitly the plasticity near grain boundaries. Consequently, the ultimate objective of the work was to establish a link between intergranular brittleness and the interaction between dislocations and grain boundaries. In this way, the macroscopic mechanical properties of a number of ordered compounds are explained in terms of the atomic structure present in these materials.

Indeed, there is experimental evidence that in $Ni_3Al$ the dislocation mobility in the vicinity of grain boundaries may be strongly enhanced when ductilization takes place [2] and that plastic flow precedes intergranular fracture [3]. Considering these experiments, it might be reasoned that the passage of gliding dislocations arriving from the lattice can be hindered by grain boundaries.

## 2. Experiments

### 2.1. Computer modelling experiments

In the modelling study, Finnis-Sinclair potentials representing $Ni_3Al$ [4] were used for the description of interatomic forces. For the simulations, the following procedure was used. First, the grain boundary was

0921-5093/93/$6.00 

relaxed, using a standard gradient method; details are given elsewhere [5]. Secondly, a computational block for the relaxation of the dislocation near the grain boundary was constructed. The computational block of the relaxed grain boundary was extended, according to the periodicity of the CSL, to form a block of more than 40 $b \times 40$ $b$ ($b$ is the magnitude of the Burgers vector) perpendicular to the dislocation line. Next, the displacement field of a 1/2 [110] dislocation was imposed with its elastic centre initially positioned at such a distance from the grain boundary that there was no strong effect of the grain boundary on the relaxation of the dislocation core. Along the dislocation line, periodic boundary conditions were applied. The anisotropic elastic solution (as if there were only one grain present) was used for the boundary conditions perpendicular to the dislocation line. The displacement field of a 1/2 [110] superpartial was imposed with its elastic centre near the boundary plane, connected by a ribbon of antiphase boundary (APB) to another superpartial at elastic equilibrium distance, according to the APB energy. The initial position of the core was always chosen such that dissociation would occur on the glide plane [6, 7]. The dislocation–grain boundary relaxation was carried out in the usual way for dislocation relaxation [8].

After relaxation of the dislocation core, a homogeneous shear strain was imposed on the computational block, corresponding to a shear stress, as prescribed by anisotropic elasticity theory (as if only the grain initially containing the dislocation were present). The shear stress was applied in the direction of the Burgers vector, such that the dislocation would move towards the grain boundary plane. The simulations started by imposing a shear strain corresponding to a small stress. Larger stresses were built up by repeating this process.

### 2.2. *In situ deformation*

$Ni_3Al$ was prepared by arc-melting 99.99% pure nickel and 99.999% pure aluminium. The material was homogenized at 1100 °C (1373 K) for 5 days, resulting in grain sizes of 1 mm. Miniature tensile specimens ($6 \times 3$ mm$^2$, with a thickness of 350 $\mu$m) were cut out of the bulk material by spark erosion. There were two holes in the sample through which it was held by the pins of the two grips of the deformation holder. The sample was necked in the middle, so as to maximize the likelihood that the deformation would start near the future electron transparent region. Care was taken to have a grain boundary, preferably a coherent twin boundary, present in the middle of the sample.

Next, the sample had to be thinned, to obtain an electron transparent region. First, the sample was ground to a thickness of 150 $\mu$m using a Gatan disc grinder and then the sample was dimpled on both sides at the location of the grain boundary, reducing the thickness locally from 150 $\mu$m to around 60 $\mu$m. This was done to increase the probability of having the grain boundary in the thin area. The last step of the preparation process was thinning of the specimen in a Struers Tenupol electropolishing unit, using a mixture of 70% methanol and 30% nitric acid at 0 °C, at an applied voltage of 8 V.

For observation of the specimen, a JEM 200-CX was used, which was operated at 200 kV. The specimen was mounted in a special single tilt *in situ* deformation holder, built according to principles taken from Kubin and Veyssière [9]. In the deformation holder, the sample is strained by a vacuum system, which is operated from outside the microscope. In this way the sample is deformed at constant load. The processes during deformation could be monitored by a TV-system and could be recorded on video. The deformation was stopped before total disruption of the specimen. After the *in situ* deformation, specimens that promised to be interesting were shaped into 3 mm diameter discs by very cautious grinding, taking care that the thin area was protected. In this way they fitted in a double tilt holder and the defects could be analysed in detail.

## 3. Results

### 3.1. *Computer modelling*

In particular the interaction of a 1/2 [110] dislocation of pure screw character with the $\Sigma = 3$ $(\bar{1}11)$ ($\Theta = 109.47°$ around [110]) coherent twin boundary was simulated. In this set-up, transmission of the dislocation through the grain boundary is relatively easy, as no residue is left behind in the grain boundary plane. In the following, all Miller indices are in the coordinate system of the upper grain, unless indicated otherwise. In the kinematic simulations, the shear stress was applied to the $(1\bar{1}1)$ plane.

It has to be emphasized that the symbols indicating the atom positions are drawn as if there is no dislocation present. The results for the kinematic simulations are depicted using the differential displacement method [10]. This method indicates the relative displacement of each atom with respect to its neighbours in a certain crystallographic direction (usually the direction of the Burgers vector). If the absolute value of the relative displacement exceeds half of the periodicity of the lattice in that direction (here 1/2 [110] was used), an integer number times the period is added or subtracted. The position of the APB is indicated by a line. The relative displacements are indicated by arrows drawn between the atoms.

The $\Sigma = 3$ boundary acted as an obstacle to dislocation motion. The leading 1/2 [110] superpartial dislocation was dissociated into two Shockley partials with very small separation. Upon arrival at the boundary plane, the leading Shockley partial was delayed and a slight decrease in separation of the Shockleys could be observed. The trailing 1/2 [110] superpartial dislocation also approached the leading dislocation. When the shear stress reached a level of 4 times the friction stress (the stress needed to start motion of the dislocation in perfect lattice 250 MPa for copper, 200 MPa for $Cu_3Au$, 350 MPa for $Ni_3Al$), transmission occurred across the boundary into the symmetric slip plane $(1\bar{1}\bar{1})_{II}$ in the other grain, see Fig. 1. Transmission occurred at 1.6 times the friction stress for copper, at 2 times the friction stress for $Cu_3Au$ and at 4 times the friction stress for $Ni_3Al$, indicating that the $\Sigma = 3$ boundary is a stronger obstacle to dislocation movement in $Ni_3Al$.

In general the results of computer modelling studies [11, 12] indicate that grain boundaries in $L1_2$ ordered compounds hinder dislocation motion. This effect increases with higher ordering tendency. A typical example to illustrate this point is presented in Fig. 2. When the leading 1/2 [110] superpartial reached for example a $\Sigma = 27$ boundary, it was halted, with one Shockley merged in the boundary plane and one Shockley in the lattice, very close to the boundary plane. When the stress level increased, the Shockley partial in the lattice gradually spread its core onto the $(\bar{1}11)$ plane. At a stress level of 1700 MPa, the Shockley partial (originally 1/6 [121]) had dissociated into a 1/6 $[\bar{1}10]$ stair rod dislocation (this type of dislocation is frequently observed as the connection between two stacking faults on different {111} planes), located approximately at the original position of the Shockley, and a new Shockley partial, 1/6 [211], which had merged into the right part of structural unit no. 2. In this way, a new, second region of complex stacking fault (CSF) had formed on the $(\bar{1}11)$ plane, connecting the stair rod dislocation and the newly formed Shockley partial, see Fig. 2(a). At a stress level of 1950 MPa, the trailing 1/2 [110] superpartial approached the configuration and a reaction between the stair rod dislocation and the leading Shockley of this superpartial took place, in which the 1/6 $[12\bar{1}]$ Shockley partial was created. This 1/6 $[12\bar{1}]$ Shockley partial cross-slipped away along the $(\bar{1}11)$ plane, thus creating an APB on the $(\bar{1}11)$ plane. Finally, at a stress level of 2100 MPa, a CSF was formed on a $(1\bar{1}\bar{1})_{II}$ plane (where II indicates the coordinate system of the lower grain) in the other grain, see Fig. 2b). In copper, transmission is observed at a stress level of less than 3 times the friction stress, while in $Ni_3Al$ the leading superpartial dislocation only enters the boundary at a very high stress level. At 6 times the friction stress a complicated reaction takes place and transmission occurs at a different location in the grain boundary.

### 3.2. In situ deformation

In many samples, cracks (some of which were already present before the deformation started) were

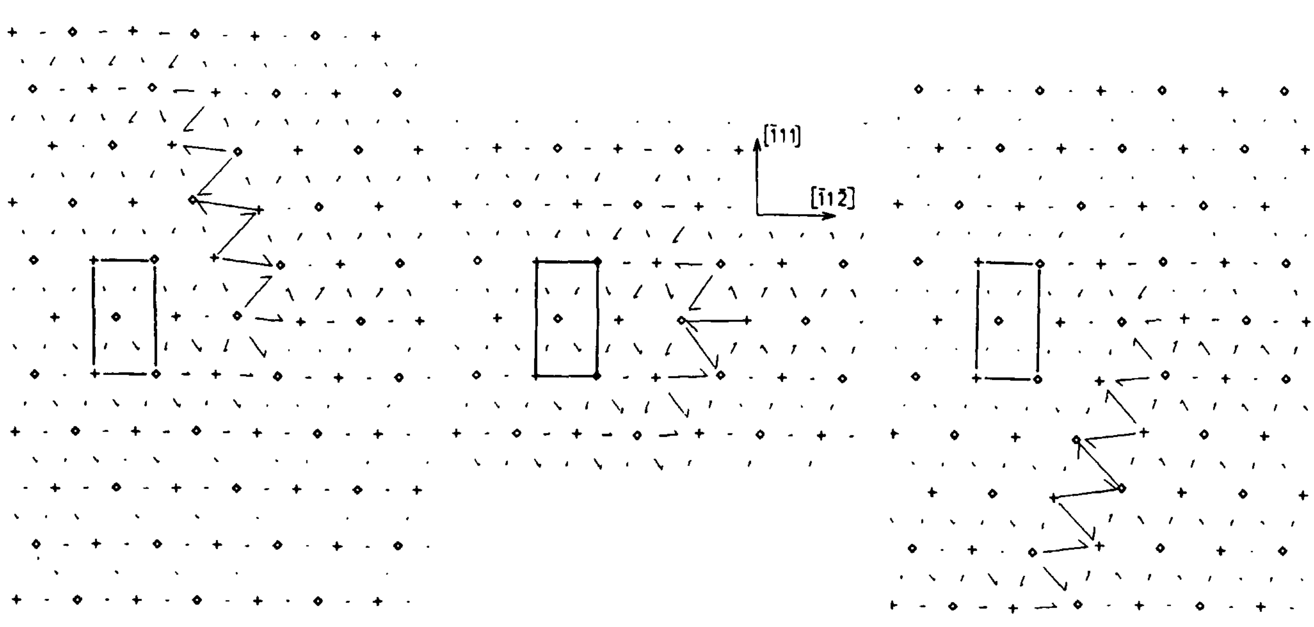


Fig. 1. (a)–(c) Three stages of the transmission through the $\Sigma = 3$ boundary of a unitary $1/2\langle 110\rangle$ screw dislocation (a projection along [1 1 0] is shown). The heights indicated by the symbols are heights before the dislocation was imposed.

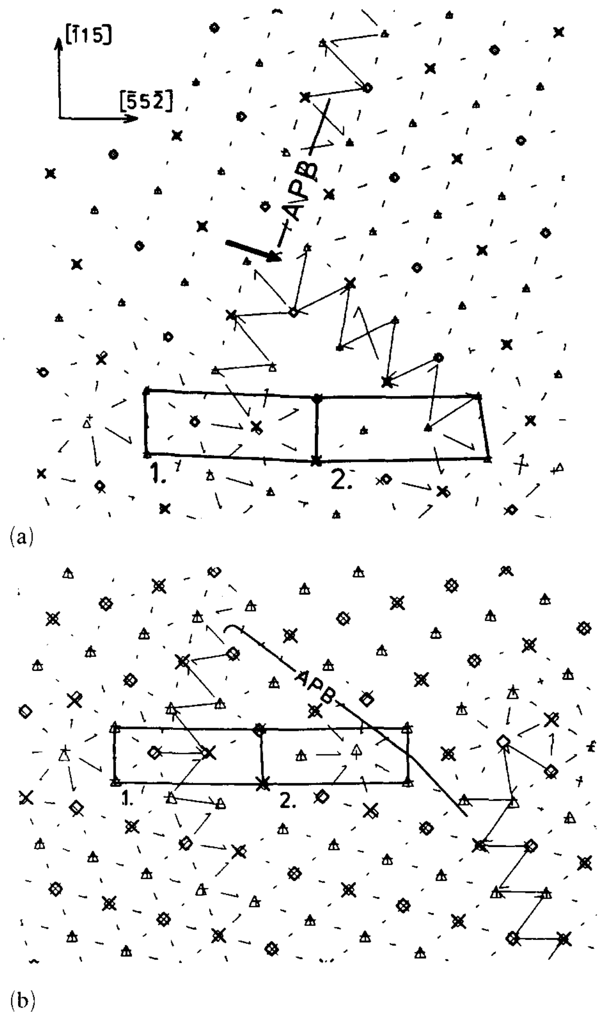


Fig. 2. Interaction between the screw dislocation and the $\Sigma = 27$ boundary in the kinematic simulations in $Ni_3Al$. The different symbols indicate different heights in the order □, +, x, △. The aluminium atoms are indicated by thicker lines. (a) First stage of the interaction (1700 MPa). Both the leading and the trailing superpartial dislocations are visible. The arrow indicates the position of the stair rod dislocation. (b) Final configuration (2100 MPa). The trailing superpartial has cross-slipped to the right and a CSF has been created in the lower grain.

observed that had initiated at the edge of the thin foil, propagating along $\{111\}$ planes. Dislocations were often seen to be emitted from the crack tip, at the plane of the crack and sometimes also on inclined planes. In addition, observations were made of dislocations arriving from the bulk, although these observations were not so numerous. The dislocations from the bulk never arrived all on the same slip plane, but seemed to appear in slip bands. Quite frequently, the propagation of the crack occurred in a jerky type of motion and then it was impossible to observe any dislocation motion.

In many of the specimens there was a grain boundary, often a coherent twin boundary ($\Sigma = 3$, 109.47° around [110] with boundary plane $(\bar{1}11)$), visible in the electron transparent region. A number of observations were made of individual dislocations that had been emitted from cracks. Sometimes dislocations arriving from the bulk impinged on twin boundaries and were arrested at the boundary plane. Cracks were seen that had grown through a twin boundary and had changed their direction of propagation upon crossing the boundary plane.

One sample showed a crack which had grown during the *in situ* deformation to the close vicinity of a coherent twin boundary, but which had not crossed the boundary (Fig. 3). On the other side of the boundary, starting exactly from the line of intersection of the crack plane and the boundary plane, slip traces could be observed leading into the other grain, to a large number of dislocations that all had the same slip plane (Fig. 4).

This sample was chosen for further analysis in the double tilt holder. The rotation of the boundary under study could be described within the error margins as a 109.5° rotation around [1 1 0], characteristic for a twin boundary. By tilting to an edge-on position, the boundary plane was determined to be $(\bar{1}11)$, which is equal to $(\bar{1}1\bar{1})_{\mathrm{II}}$. The index II indicates the coordinate system of the grain containing the dislocations. The grain containing the crack is meant if no index is used. In a similar way, the plane of the crack was determined to be close to $(1\bar{1}1)$ and the slip plane of the dislocations was determined to be $(1\bar{1}\bar{1})_{\mathrm{II}}$. By the $\boldsymbol{g}\cdot\boldsymbol{b}=0$ invisibility criterion, the Burgers vector of the dislocations was determined to be parallel to $[110]_{\mathrm{II}}$; this is the [110] direction that is common to both grains. The line direction was determined to be $[230]_{\mathrm{II}} \pm 13°$, which is close to the $[110]_{\mathrm{II}}$ screw direction. Apparently the crack propagation occurred in mode −III (tearing) producing screw dislocations.

## 4. Discussion and conclusions

The results of the transmission electron microscopy (TEM) work show that cracks may emit dislocations parallel to their own plane during propagation. In the case of the sample containing a twin boundary that was analysed in detail, the plane of the crack crossed a coherent twin boundary ahead of the crack and it might be envisaged that a number of dislocations were emitted from the crack tip in the $(1\bar{1}1)$ plane and impinged on the boundary. The slip traces emanating on the other side of the boundary indicate that a number of dislocations have emerged from the boundary in the $(1\bar{1}\bar{1})_{\mathrm{II}}$ plane exactly at the point where the plane of the crack intersects with the boundary plane. Thus, it is probable that these dislocations have been emitted from the crack tip and have been transmitted through the grain boundary. As the [110] direction is common to both grains, the Burgers vector could remain the same in both grains and no residue is left in the boundary. The line vector in parallel to the intersection of the crack plane and the outgoing slip plane and thus transmission could occur without rotation of the dislocation line in the boundary plane. The large number of dislocations may indicate that there was a large force on the leading dislocation of a pile-up in front of the boundary, necessary to cause transmission of the dislocations to the other grain. Grain boundary sources of course cannot be ruled out completely as origin of the observed dislocations. However, very often, if operation of grain boundary sources is observed, dislocations are generated on many different slip planes [13] (our own observations of two other samples indicate the same), while here all the dislocations are on one slip plane.

Our experimental observations of the interaction with the $\Sigma = 3$ coherent twin boundary can be compared with the computer modelling results, see also refs. 11 and 12. The dislocation–grain boundary system studied is exactly the same as the system that is studied here experimentally and therefore a one-to-one comparison is possible. The interaction mechanism observed in $Ni_3Al$ in the simulations is the same as that which was observed in the *in situ* deformation experiment. The magnitude of the stress at which transmission occurs cannot be compared so easily, as there is no experimental observation of a pile-up of dislocations against the grain boundary. From the number of dislocations in a pile-up and their spacing, the effective stress on the first dislocation near the boundary plane can be calculated. The friction stresses observed in the simulations are high in comparison with experiment and therefore the stresses necessary for transmission can be expected to be high as well.

Fig. 3. Crack that has grown very close to a $\Sigma = 3$ coherent twin boundary and slip lines on the other side of the boundary: 1 crack, 2 boundary plane, 3 slip lines.

The main feature of $Ni_3Al$ as compared with f.c.c. and other $L1_2$ materials such as $Cu_3Au$ lies in the stress level at which transmission through the boundary occurs [11]. The two superpartial dislocations in $L1_2$ constituting the arriving dislocation will decrease their separation in response to the applied stress, when the leading superpartial dislocation is halted at the boundary. In this way stress concentrations near the boundary will be generated which will increase upon increasing ordering tendency. Since the ordering tendency in $Ni_3Al$ is much larger than in $Cu_3Au$, the boundary in $Ni_3Al$ will act as a much stronger obstacle for dislocation transmission. The modelling results obtained indicate that the interaction between lattice dislocations and grain boundaries is essential to explain the intergranular fracture occurring in a number of ordered compounds, in particular those with a high ordering energy.

Finally, one should be careful in generalizing our results obtained for all $L1_2$ ordered systems. Indeed, as the mechanical properties of more $L1_2$ materials are investigated experimentally, it is found that several are intrinsically brittle because of intergranular failure as in

Fig. 4. The dislocation configuration found attached to the slip lines (the marker shows 100 nm): 1 crack, 2 boundary plane, 3 dislocation array.

$Ni_3Al$. However, it has to be emphasized that in intermetallics, for example, $Al_3Ti$, cleavage fracture is also found to be the failure mode, rather than intergranular failure. In cleavage fracture it is feasible that there is a mechanism for crack tip plasticity which does not require macroscopic dislocation motion at all [14].

## References

1 K. Aoki and O. Izumi, *Nippon Kinzaku Gakkaishi, 43* (1979) 1190.
2 I. Baker, E. M. Schulson and J. A. Horton, *Acta Metall. Mater., 35* (1987) 1533.
3 S. Hanada, T. Ogura, S. Watanabe, O. Izumi and T. Masumoto, *Acta Metall. Mater., 34* (1986) 13.
4 V. Vitek, G. J. Ackland and J. Cserti, in G. M. Stocks, D. P. Pope and A. F. Giamei (eds.), in *Alloy Phase Stability and Design, Mater. Res. Soc. Symp. Proc., 186* (1991) 237.
5 A. P. Sutton and V. Vitek, *Philos. Trans. R. Soc. London, Ser. A, 309* (1983) 37.
6 D. Farkas and E. J. Savino, *Scripta Metall. Mater., 22* (1988) 557.
7 M. Yamaguchi, V. Paidar, D. P. Pope and V. Vitek, *Philos. Mag. A, 45* (1982) 867.
8 Z. S. Basinski, M. S. Duesbery and R. Taylor, *Philos. Mag., 21* (1970) 1201.
9 L. P. Kubin and P. Veyssière, *Proc. 10th Int. Congress on Electron Microscopy, Hamburg, Germany*, Deutsche Gesellschaft für Elektronenmikroskopie, (Battelle-Institut) Frankfurt am Main, 1982, p. 531.
10 V. Vitek, R. C. Perrin and D. K. Bowen, *Philos. Mag., 21* (1970) 1049.
11 B. J. Pestman, J. Th. M. De Hosson, V. Vitek and F. W. Schapink, *Philos. Mag., A, 64* (1991) 951.
12 B. J. Pestman, J. Th. M. De Hosson and V. Vitek, F. D. Tichelaar and F. D. Schapink, in G. M. Stocks, D. P. Pope and A. F. Giamei (eds.), in *Alloy Phase Stability and Design, Mater. Res. Soc. Symp. Proc., 186* (1991) 253.
13 G. M. Bond, I. M. Robertson and H. K. Birnbaum, *J. Mater. Res., 2* (1987) 436.
14 M. L. Jokl, V. Vitek, C. J. McMahon and P. Burgers, *Acta Metall. Mater., 37* (1989) 87.